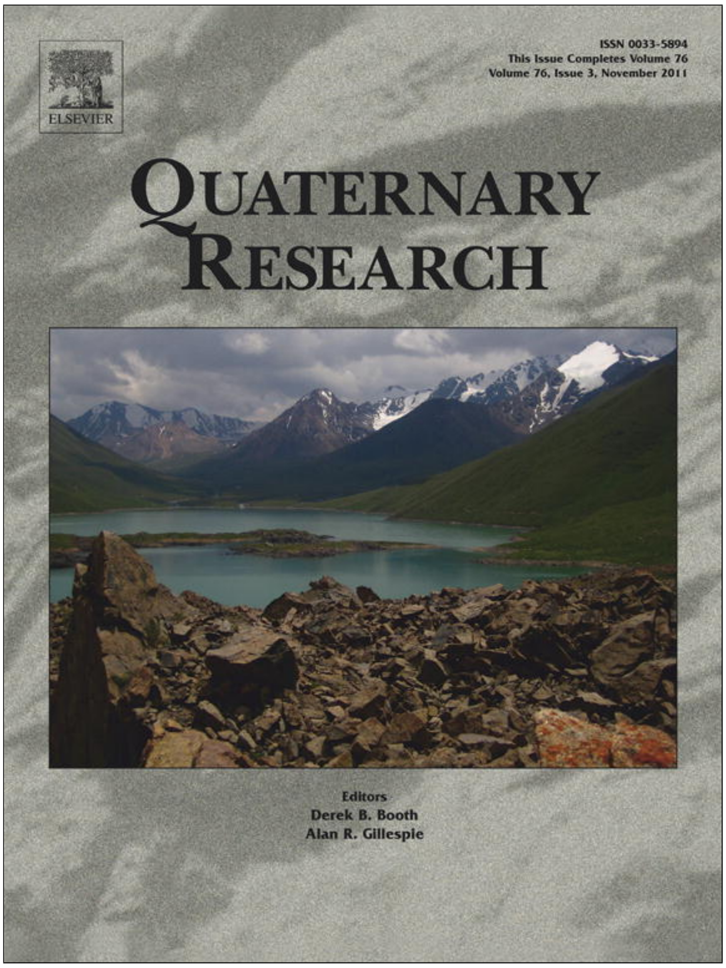
ISSN 0033-5894
This Issue Completes Volume 76
Volume 76, Issue 3, November 2011
ELSEVIER
QUATERNARY RESEARCH
Editors
Derek B. Booth
Alan R. Gillespie

Quaternary Research 76 (2011) 401–410

Contents lists available at ScienceDirect

Quaternary Research

journal homepage: www.elsevier.com/locate/yqres

Deglaciation, basin formation and post-glacial climate change from a regional network of sediment core sites in Ohio and eastern Indiana

Katherine C. Glover [a,*], Thomas V. Lowell [a], Gregory C. Wiles [b], Donald Pair [c], Patrick Applegate [d], Irena Hajdas [e]

[a] Department of Geology, University of Cincinnati, Cincinnati, OH 45221-0013, USA
[b] Department of Geology, The College of Wooster, Wooster, OH 44691, USA
[c] Department of Geology, University of Dayton, Dayton, OH 45469-2364, USA
[d] Department of Physical Geography and Quaternary Geology, Stockholm University, S-106 91 Stockholm, Sweden
[e] PSI/ETH Laboratory for Ion Beam Physics, Schafmattstr. 20 HPK H27, CH-8093 Zurich, Switzerland

ARTICLE INFO

Article history:
Received 23 August 2010
Available online 3 August 2011

Keywords:
Last Glacial Maximum
Termination 1
Ohio
Indiana
Midwest
Radiocarbon dating
Post-glacial
Lacustrine deposit
Greenland
Deglaciation

ABSTRACT

Many paleoclimate and landscape change studies in the American Midwest have focused on the Late Glacial and early Holocene time periods (~16–11 ka), but little work has addressed landscape change in this area between the Last Glacial Maximum and the Late Glacial (~22–16 ka). Sediment cores were collected from 29 new lake and bog sites in Ohio and Indiana to address this gap. The basal radiocarbon dates from these cores show that initial ice retreat from the maximal last-glacial ice extent occurred by 22 ka, and numerous sites that are ~100 km inside this limit were exposed by 18.9 ka. Post-glacial environmental changes were identified as stratigraphic or biologic changes in select cores. The strongest signal occurs between 18.5 and 14.6 ka. These Midwestern events correspond with evidence to the northeast, suggesting that initial deglaciation of the ice sheet, and ensuing environmental changes, were episodic and rapid. Significantly, these changes predate the onset of the Bølling postglacial warming (14.8 ka) as recorded by the Greenland ice cores. Thus, deglaciation and landscape change around the southern margins of the Laurentide Ice Sheet happened ~7 ka before postglacial changes were felt in central Greenland.

Introduction

During the Last Termination (22–11 ka), the Earth system changed to a new state in which land ice cover was relatively restricted. Because this change provides a backdrop for the present interglacial period and a template for prior glacial terminations, interest in this long-studied time period continues (e.g., Anderson et al., 2009; Cheng et al., 2009; Clark et al., 2009; Denton et al., 2010).

Emerging records show that the pattern of change during the Last Termination was complex. In the Southern Hemisphere, full-glacial conditions persisted until ~17.5 ka, when deuterium in Antarctic ice cores began to rise and the Southern oceans began upwelling (Anderson et al., 2009). In the Northern Hemisphere, oxygen isotopes in Greenland show only gradual change between 23.3 and 14.8 ka (Andersen et al., 2006; Rasmussen et al., 2006; Svensson et al., 2008), followed by the well-studied Late Glacial oscillations of the Bølling/Allerød (B/A; 14.7–12.7 ka; Denton et al., 2010) and Younger Dryas (YD; 12.8–11.5 ka, Denton et al., 2010).

In contrast to high-latitude records from ice cores, the timing of initial change may differ significantly around the midlatitude margins of the former ice sheets. The Laurentide Ice Sheet, in particular, reached 40°N, more than halfway to the equator. It is unclear whether the poles should lead, lag, or be in phase with these low-latitude margins; polar amplification would suggest that the poles should experience warming sooner than lower latitudes, but perhaps the poles were temporarily buffered from changes that happened first at lower latitudes.

Here, we use a network of radiocarbon-dated sediment cores from small bogs and wetlands to show that initial retreat of the Laurentide margin from its local Last Glacial Maximum extent was largely complete before significant warming was detected in the ice cores. Various efforts over the past decade (Heusser et al., 2002; Glover, 2004; Pritchard, 2006; and the 2001–2002 Summer Keck Geology Consortiums) have accumulated a network of lacustrine sequences. In this paper, we report results from 29 new sites from the mid-latitudes of North America (Fig. 1, Table 1). The combined data set includes 52 sites with 81 radiocarbon dates. All these sites have basal dates defining the deglaciation pattern of the region. The pace and style of post-glacial landscape change is also of interest. Many cores from the formerly glaciated landscape show lithologic transitions significantly upsection of the basal contact. We dated these transitions to examine regional patterns of postglacial landscape change.

* Corresponding author at: Department of Geography, UCLA, Los Angeles, CA 90095-1524.
E-mail address: kcglover@ucla.edu (K.C. Glover).

0033-5894/$ – see front matter © 2011 University of Washington. Published by Elsevier Inc. All rights reserved.
doi:10.1016/j.yqres.2011.06.004

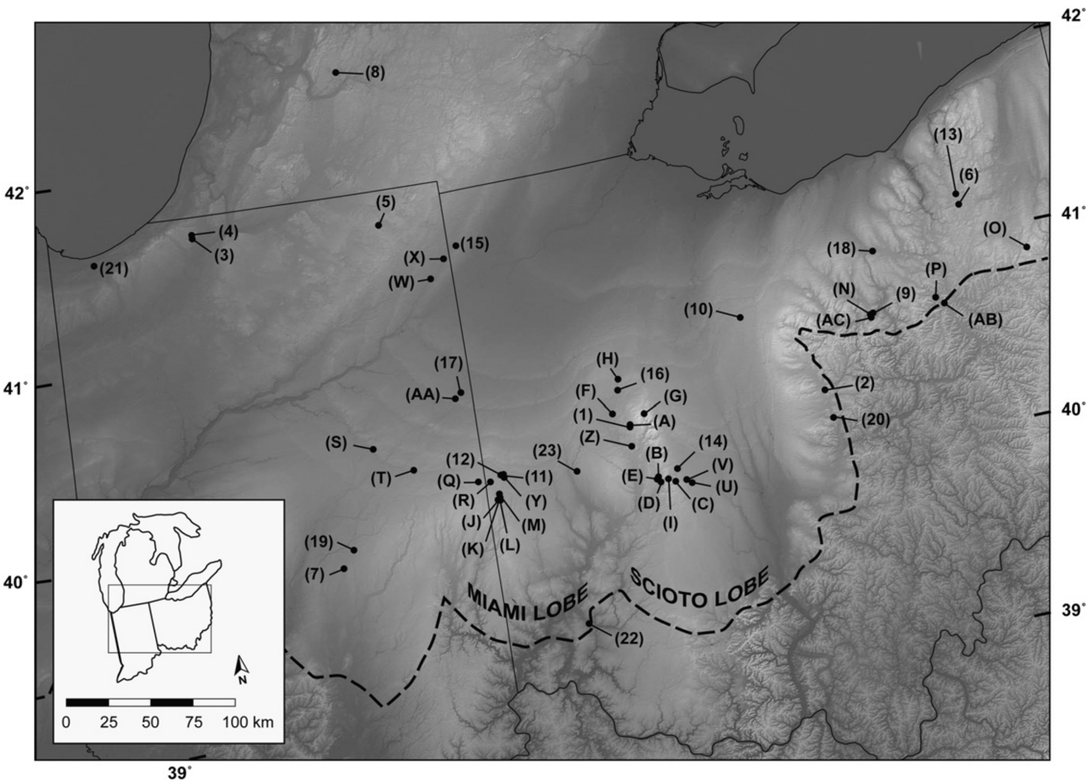

Figure 1. Digital Elevation Map of Ohio, Indiana and Michigan, with lake and relict basin sites that have been cored and radiocarbon dated. Numbered sites represent prior, published work (see Table 1). Sites indicated by letters are new data. The dashed line represents the maximum limit of the most recent glaciation.

Finally, we assess the utility of radiocarbon-based chronology as a means of tracking deglaciation. Radiocarbon dates on samples found in postglacial depressions must postdate ice retreat from the overlying land surface. It has been commonly pointed out (e.g. Porter and Carson, 1971; Clayton and Moran, 1983) that there may be a time lag between the uncovering of the landscape, and the accumulation of organic remains. Conversely, some studies have successfully employed bog-bottom dating to reconstruct deglaciation (e.g. Lowell, et al., 1995; Denton, et al., 1999). We argue that a network, rather than isolated sites, yields more robust insight to deglaciation and later environmental change for a larger region.

Methods

Sediment core recovery and analysis from 52 lakes and relict basins in eastern Indiana and central Ohio provide the basis for this study. This data set included 23 published sites, including post-glacial lakes and bogs (numbered sites, Table 1; Fig. 1), and 29 sites first reported here (alphabetic sites, Table 1; Fig. 1). Many of the published sites are included in comprehensive regional analyses (Ogden, 1966; Bailey, 1972; Williams, 1974; Shane, 1975; Whitehead et al., 1982; Overpeck et al., 1985; Shane, 1987; Shane 1989; Shane and Anderson, 1993; Hinnefeld, 1996; Singer et al., 1996; Table 1). Basal dates, where available, are included. New sites were recovered during Keck Consortium undergraduate research summer initiatives in 2001–2002, and other related projects (Glover, 2004; Pritchard, 2006). Several of these sites were targeted because they lie in the slightly higher terrain of west-central Ohio, which represents an interlobate region between Laurentide Ice Sheet's Miami and Scioto sublobes.

Most of these prior studies include pollen analysis, and are from lakes or bogs that were selected to recover as long a record as possible. However, for the new sites, our focus was on deglaciation; thus, several of these sites were relict bogs and wetlands with only shallow or seasonal standing water, and the core sequences were truncated. In other words, organic materials were no longer accumulating at many of the sites, and they record the early but not latest history.

Sites were cored with a Livingstone piston corer, close to the basin center. Typically, two overlapping cores were taken. In most cases, the bottom layer of the core consisted of poorly sorted, inorganic sediment, or a layer of stiff clay (Fig. 2a). Repeated coring allowed interpolation over gaps between core segments. The cores were described and photographed according to standard methods.

We measured magnetic susceptibility and loss on ignition (550°C and 1000°C; Dean, 1974) at 2-cm intervals in each core. High magnetic susceptibility generally indicates a clastic, inorganic deposition that is typical of a freshly deglaciated landscape. High loss on ignition values indicate the presence of organic matter (at 550°C) or carbonate (at 1000°C). Where organic macrofossils were available, at least two horizons in each core were radiocarbon dated: the lowermost part of the sediment (indicating a minimum for the time of basin formation), and the first major sedimentary transition upsection. These are referred to here as "basal dates" and "transition dates," respectively. Macrofossils such as twigs and seeds were often found in the glacial debris at the bottom of each core.

For the transition dates, macrofossils were recovered from as close to the contact as possible and this was typically in the upper unit (Fig. 2a). Many of the sequences show a shift from silt or clay accumulation to material of greater organic content, such as peat or gyttja. In prior studies, transitions were identified by major shifts in pollen species and organic content. In particular, the decline of *Picea* (spruce) species is seen as a transition to warmer climates for the region (Shane and Anderson, 1993).

The exact nature of this transition varied between individual basins, as it is controlled by several local factors (e.g., geomorphic setting, nearness to the ice margin, local vegetation) that can affect the organic flux and sedimentation rate into the basin. Thus, only

Table 1
Location of bog and lake sites in Ohio and Indiana that formed after the LGM, including basal dates. For new sites, macrofossil material (e.g. twigs, seeds) was submitted for AMS radiocarbon dating. Shaded sites are those that formed between 20 and 17.2 ka, a major phase of deglaciation for the region.

Site no.	Site name	Lat., long.	Lab number	Basal age (^{14}C year BP)	Median age (cal year BP)	Age range (cal year BP)	2σ Probability	Reference
Prior Work								
1	Silver Lake	30.350, – 83.800	OWU – 39	10,778 ± 210	12,680	13,125 – 12,133	1.0000	Ogden 1966
2	Torren's	40.350, – 82.467	OWU – 219	12,800 ± 600	15,300	16928 – 13597	1.0000	Ogden 1967
3	Clear Lake	41.650, – 86.530	IU – 143	13,300 ± 300	16,100	16,920 – 15,100	1.0000	Bailey1972
4	Hudson Lake	41.670, – 86.530	IU – 133	11,500 ± 400	13,390	14,517 – 14,305	0.9823	Bailey1972
5	Pretty Lake	41.583, – 85.250	OWU – 242	13,265 ± 520	15,940	17,380 – 17,330	0.9954	Williams 1974
6	Battaglia Bog	41.144, – 81.329	ISGS – 252	15,570 ± 340	18,790	19,425 – 18,407	0.8637	Shane 1975, 1987
7	Christensen Bog	39.867, – 85.825	(not given)	13,820 ± 80	16,920	17,137 – 16,736	1.0000	Whitehead 1982
8	Wintergreen L.	42.398, – 85.383	WIS – 676	13,195 ± 125	16,060	16,665 – 15,253	1.0000	Overpeck 1985
9	Brown's Lake	40.680, – 82.063	SI – 1361	16,680 ± 1240	20,020	22,951 – 22,761	0.9924	Shane 1987
10	Bucyrus Bog	40.797, – 82.933	ISGS – 1664	17,240 ± 340	20,560	21,400 – 19,796	0.9705	Shane 1989
11	Carter Site	40.217, – 84.681	DIC – 243	14,810 ± 170	18,050	18,544 – 17,602	1.0000	Shane 1987
12	Stotzel-Leis Site	40.217, – 84.689	DIC – 510	14,890 ± 130	18,190	18,547 – 17,765	1.0000	Shane 1987
13	East Twin Lake	41.199, – 81.333	WIS – 2048	13,660 ± 140	16,790	17,114 – 16,384	1.0000	Shane; Anderson 1993
14	Fudger Lake	40.100, – 83.533	CAMS – 2409	11,680 ± 90	13,540	13,753 – 13,334	1.0000	Shane; Anderson 1993
15	Ladd Lake	41.417, – 84.750	ISGS – 1679	14,680 ± 310	17,860	18,569 – 17,123	1.0000	Shane; Anderson 1993
16	Neville Marsh	40.546, – 83.833	ISGS – 1677	12,210 ± 150	14,160	14,910 – 13,766	1.0000	Shane; Anderson 1993
17	Pyle Site	40.667, – 84.883	ISGS – 1055	13,510 ± 160	16,600	16,993 – 15,853	0.9804	Shane; Anderson 1993
18	Quillin Site	41.000, – 81.967	ISGS – 402	14,500 ± 150	17,630	18,026 – 17,141	1.0000	Shane; Anderson 1993
19	Rhule Fen	39.954, – 85.742	ISGS – 1658	12,660 ± 130	14,920	15,535 – 14,197	1.0000	Shane; Anderson 1993
20	Smoot Lake Bog	40.206, – 82.446	ISGS – 1171	14,350 ± 310	17,480	18,467 – 18,304	0.9651	Shane; Anderson 1993
21	Portage Lake	41.576, – 87.223	GX – 20208AMS	10,400 ± 160	12,230	12,633 – 11,700	0.9923	Singer 1996
22	Bunnel Road	39.394, – 84.286	Beta – 72287	18,460 ± 90	22,050	22,343 – 21,571	1.0000	Hinnefeld 1996
23	0445 – Hartzwell	40.173, – 84.194	ETH – 30202	15,710 ± 90	18,850	19,275 – 19,062	0.8596	Pritchard 2006
This study								
A	0101 – TechPlant	40.359, – 83.792	Beta – 158291	11,860 ± 270	13,740	14,793 – 14,760	0.9962	
B	0103 – FarmPond	40.075, – 83.668	AA – 45069	15,810 ± 140	19,020	19,386 – 18,709	1.0000	
C	0104 – ClydeSite	40.033, – 83.561	AA – 45069	15,350 ± 100	18,610	18,846 – 18,477	0.9324	
D	0105 – GloryHole	40.064, – 83.653	AA – 45073	15,503 ± 91	18,710	18,878 – 18,562	1.0000	
E	0106 – Murphy'sBog	40.064, – 83.675	AA – 45074	14,986 ± 98	18,251	18,560 – 17,952	1.0000	
F	0107 – Stevenson	40.431, – 83.896	AA – 45077	14,360 ± 120	17,460	17,876 – 17,078	1.0000	
G	0108 – Bellfontaine	40.406, – 83.684	AA53435	15,564 ± 88	18,750	18,909 – 18,589	1.0000	
H	0109 – Mike's Place	40.600, – 83.178	AA – 45078	14,600 ± 91	17,760	18,047 – 17,371	0.9854	
I	0201 –Mechanicsburg	40.051, – 83.603	AA – 45079	16,170 ± 97	19,300	19,541 – 19,514	0.9853	
J	0202 – Nashville	40.093, – 84.743	AA53419	15,869 ± 91	19,090	19,383 – 18,819	1.0000	
K	0203 – Sharpeye	40.101, – 84.745	AA53425	16,400±170	19,560	20,081 – 19,238	0.9606	
L	0204 – EdgarPond	40.108, – 84.730	AA53442	16,010 ± 100	19,160	19,416 – 18,897	1.0000	
M	0205 – Wildcat Bog	40.122, – 84.730	AA53429	10,676 ± 58	12,610	12,728 – 12,533	0.9935	
N	0206 – Brown's Bog	40.682, – 82.066	AA53431	14,660 ± 83	17,830	18,438 – 18,313	0.9589	
O	0207 – Mastodon	40.854, – 80.941	AA53428	14,960 ± 82	18,260	18,546 – 17,946	1.0000	
P	0208 – Brewster Site	40.703, – 81.615	AA53439	20,930 ± 160	24,940	25,490 – 24,479	1.0000	
Q	0209 – Monroe's Bog	40.203, – 84.853	AA53418	15,640 ± 97	18,790	19,243 – 19,145	0.9713	
R	0210 – Hunt's Bog	40.191, – 84.775	AA53423	16,128 ± 90	19,260	19,448 – 18,928	1.0000	
S	0301 – Cook's Bog	40.453, – 85.514	Beta – 182975	15,530 ± 60	18,730	18,874 – 18,591	1.0000	
T	0302 – Alpaca Site	40.312, – 85.271	Beta – 190862	15,540 ± 80	18,730	18,889 – 18,585	1.0000	
U	0303 – Mastodon II	40.012, – 83.453	Beta – 190863	16,050 ± 90	19,180	19,424 – 18,917	1.0000	
V	0304 – Tile Site	40.033, – 83.484	ETH – 28523	15,560 ± 100	18,740	18,919 – 18,576	1.0000	
W	0305 – Hyre	41.267, – 84.947	Beta – 194054	13,690 ± 50	16,830	17,003 – 16,662	1.0000	
X	0306 – Kenan	41.367, – 83.841	Beta – 190864	13,880 ± 70	16,950	17,174 – 16,771	1.0000	
Y	Carter II	40.210, – 84.678	CAMS – 27129	15,630 ± 150	18,800	19,273 – 19,046	0.8783	
Z	Lattimer	40.251, – 83.812	CAMS – 27130	15,770 ± 80	18,918	19,301 – 18,697	1.0000	
AA	446	40.641, – 84.918	ETH – 32177	14.780 ± 100	17,990	18,510 – 18,235	0.7042	
AB	Welty	40.690, – 81.611	Beta – 181057	14,670 ± 40	17,850	18,056 – 17,577	1.0000	
AC	Long Lake	40.666, – 82.136	Beta – 265090	14890 ± 90	18,221	18,533 – 17,834	1.0000	

~56% of our sites showed evidence of a significant change in pollen species, or increase in organic matter.

Where little organic matter was available at the horizon of interest, we interpolated between bracketing radiocarbon dates to obtain an age estimate. In these cases, the sedimentation rate spanning the transition was obtained from two bracketing dates, and the time of change then calculated in radiocarbon years (see example, Fig. 2b). The 2-sigma error range is an average of the reported measurement uncertainty from the two dates that we interpolated between.

Radiocarbon dates for each grouping were converted to calendar years using Calib 6.0 and the IntCal09 calibration curve, and referenced to the year 1950 (Tables 1 and 2; Reimer et al., 2009; Stuiver and Reimer, 2010). The highest-probability 2-sigma dates from this conversion are listed in Tables 1 and 2.

To look for patterns in the timing of postglacial landscape change, we summed the probability distributions of the individual calibrated radiocarbon dates (Fig. 3; Lowell, 1995; Glover, 2004). We carried out this procedure for basal dates (Table 1) and separately for transition dates (Table 2). This approach allows us to identify common temporal events, as represented by the peaks, across a wide geographical area. When summed this way, the probability values reflect some relative strength, and the timing of key events becomes more apparent.

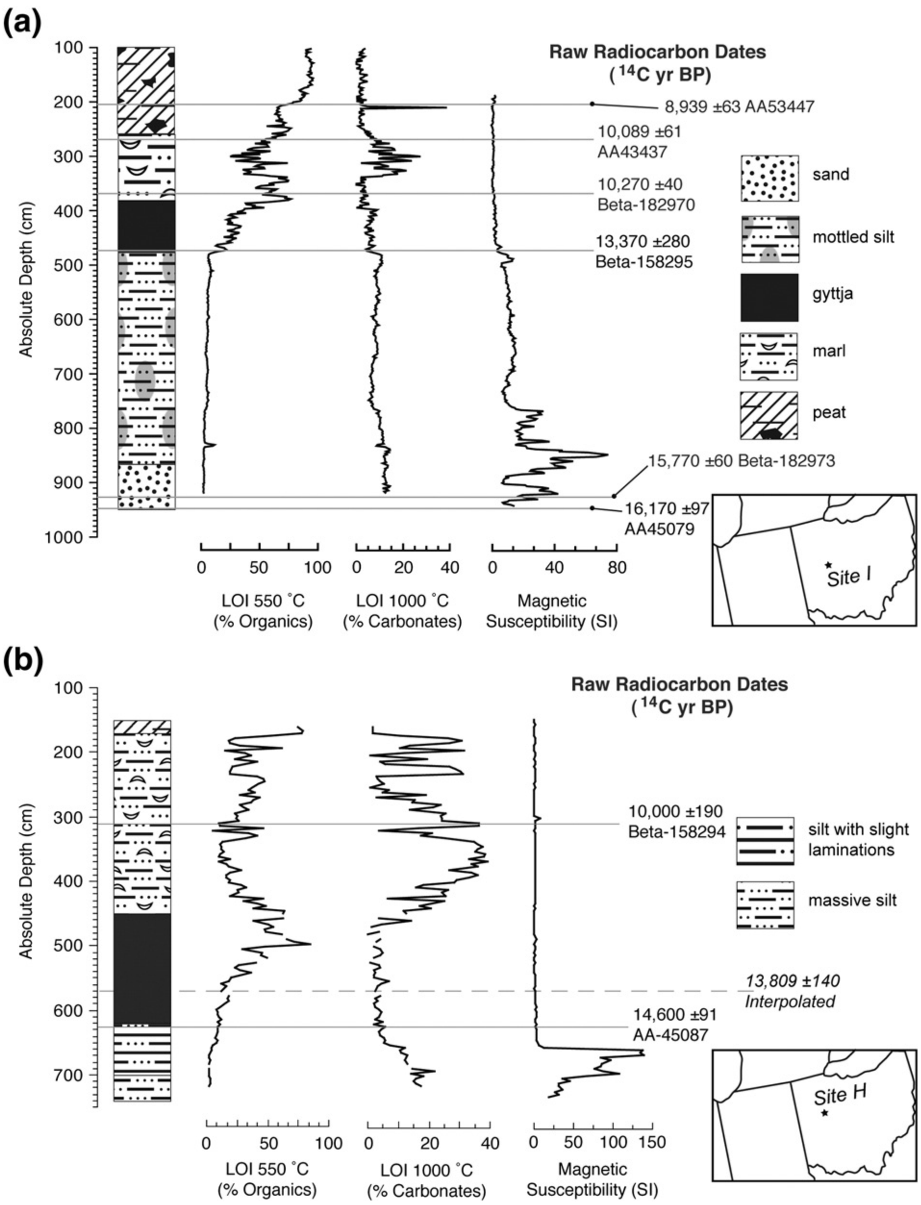

Figure 2. (a) An example of site stratigraphy from a new site (Site I, Mechanicsburg, Ohio) with both basal and transition radiocarbon dates shown. The basal date is from twigs at the lowermost level in poorly-sorted sand and gravel. The transition date marks the change from silt to gyttja sedimentation. Dates shown are in radiocarbon years, with lab number afterwards. (b) An example of a site (Site H, west of Marion, OH) from which transition time had to be interpolated from surrounding radiocarbon dates. For an interpolation, a transition was generally determined to be where the organic content began increasing.

Results

Basin formation

The oldest ages from our study represent the time of basin formation and reflect a minimum time of deglaciation. The Miami sublobe reached its maximum extent at 23.2 cal ka BP (Lowell, 1995), but the Bunnel Road Site (22), lying within 10 km of the maximum margin, formed at 22,010 ±285 cal yr BP (Beta-72287). Two more sites in northeastern Ohio (0208 Brewster Bog [P], and Bucyrus Bog [10]) formed prior to 20 ka (Fig. 1). Several other basins formed near the maximum ice sheet extent, but date to the time period 20 to 17.2 ka (Sites 9, 20, N, O, AB, AC). These sites indicate retreat of the ice margin in several sectors before 20 ka, with basins discussed below forming well inside the outer limit of the ice sheet.

At these interior sites, 20 to 17.2 ka is a time period when numerous basins formed (31 total, Table 1), suggesting widespread deglaciation that peaked at ~18.9 ka. Of the 29 sites that we found, 25 of them (86%) began organic accumulation during this time period (Table 1). These sites range across the study area from east-central Indiana to west-central Ohio (Fig. 4a), including the higher terrain in Ohio that was located between the Miami and Scioto sublobes of the Laurentide Ice Sheet. These sites lie ~100 km interior to the maximum ice-sheet extent, suggesting that the ice-sheet margin was retreating between 22.0 and 18.9 ka. Four of these sites lie in northeastern Ohio. The probability curve has a strong peak at ~18.9 ka (Fig. 3a), with many of the basal dates within only 100–200 yr of 18.9 ka and having relatively low margins of error (Table 1). Retreat at this time was geographically widespread.

Basin formation was less common for the next ~6 ka. A small pulse of basin formation occurred at 16.8 ka, concurrent with the shift from Termination 1 to Heinrich Stadial 1, and the peak of Heinrich 1 (Hemming, 2004; Fig. 3a). The decrease in basin formation indicates that the landscape had largely stabilized after 16.8 ka, and all of the sites considered in this study had been formed by 12 ka.

Table 2
Transitions observed in regional sites that suggest environmental change. AMS radiocarbon dates were based on macrofossil material; interpolations are noted below. Shaded sites indicate transitions that occurred during HS1 (18–14.6 ka). Calibrated radiocarbon dates are shown with 2-sigma values, or the 95% probability of falling within the range shown here. For dates with an asterisk (*), these denote that the authors believed there is to be a dating error, or interpolation is based upon at least one such date.

Site	Sample depth	Lab number	Transition age (^{14}C year BP)	Median age (cal year BP)	Age range (cal year BP)	2σ Probability	Nature of transition
1	610 cm	OWU – 39	9,800 ± 210	11,240	11,978 – 10,647	0.9899	Pollen transition from spruce to hardwood
19	730 cm	Interpolated	11,194 ± 130	13,070	13,317 – 12,738	1.0000	Decline of *Picea*
N	1000 cm	Interpolated	11,317 ± 71	13,210	13,364 – 13,083	1.0000	Increase in organic content
S	182 cm	Beta – 182974	11,520 ± 40	13,360	13,471 – 13,264	1.0000	Increase in organic content
15	2050 cm	ISGS – 1669	11,750 ± 180	13,600	13,970 – 13,267	1.0000	Transition from pollen zone IIa to IIb
A	550 cm	Beta – 158291	11,860 ± 270	13,740	14,605 – 13,133	0.9962	Increase in organic content
8	(not given)	(not given)	11,920 ± 770	14,110	16,687 – 12,377	0.9946	Decline of *Picea*; increase in *Pinus*
18	510 cm	ISGS – 403*	12,260 ± 90	14,180	14,654 – 13,862	0.9401	Decline of *Picea*; end of pollen zone Qu-1
16	340 cm	ISGS – 1677	12,210 ± 150	14,160	14,910 – 13,766	1.0000	Decline of *Picea*; end of pollen zone I
20	940 cm	Interpolated	12,533 ± 260	14,700	15,697 – 13,832	0.9812	Decline of *Picea*; end of pollen zone I
O	400 cm	AA53422	12,596 ± 70	14,840	15,194 – 14,435	0.9505	Transition from inorganic to organic sediment
P	530 cm	AA53416	12,740 ± 100	15,110	15,673 – 14,559	0.9850	Increase in organic content
V	360 cm	ETH – 28522	12,830 ± 85	15,310	15,948 – 14,897	0.9922	Increase in organic content; increase in magnetics
12	790 cm	Dicar 509	13,070 ± 370	15,770	16,966 – 14,468	0.9870	Decline in *Picea*; end of pollen zone Sl-1
7	~2.3 m	ISGS – 492	13,220 ± 100	16,120	16,695 – 15,388	0.9863	Base of upper peat horizon
10	212 cm	Interpolated*	13,291 ± 250	16,130	16,846 – 15,193	1.0000	End of pollen zone Bu-1, organic sed'n begins
I	462 cm	Beta – 158295	13,370 ± 280	16,210	16,933 – 15,182	1.0000	Increase in organic content
17	425 cm	ISGS – 1055	13,510 ± 160	16,600	16,993 – 15,853	0.9804	Decline in *Picea*
Q	320 cm	AA53424	13,505 ± 78	16,680	16,917 – 16,332	1.0000	Lithologic change; slight increase in organic content
6	350 cm	ISGS – 250	13,640 ± 210	16,720	17,213 – 15,846	0.9834	Decline in *Picea*
F	420 cm	Interpolated	13,760 ± 115	16,880	17,148 – 16,633	1.0000	Increase in organic content
H	570 cm	Interpolated	13,809 ± 140	16,920	17,239 – 16,602	0.9958	Increase in organic content
D	785 cm	Interpolated	13,986 ± 95	17,050	17,261 – 16,810	0.9150	Increase in organic content
22	320 cm	Beta – 73190	14,130 ± 180	17,230	17,693 – 16,824	1.0000	Transition from eolian to biological sedimentation
T	235 cm	ETH – 28521	14,410 ± 110	17,530	17,902 – 17,144	1.0000	Increase in organic content
J	280 cm	AA53430	14,588 ± 79	17,750	18,035 – 17,386	0.9936	Lithologic change
9	1190 cm	Interpolated*	14,898 ± 1080	17,940	20,423 – 14,887	1.0000	End of pollen zone Br-1
B	335 cm	Interpolated	14,902 ± 116	18,210	18,547 – 17,810	1.0000	Transition from inorganic to organic sediment
L	385 cm	Interpolated	15,164 ± 98	18,290	18,382 – 18,027	0.6026	Transition to fine-grained sedimentation

Environmental transitions

The above shows that basin formation is the first major regional environmental change. Here we assess whether regional environmental changes can have a stratigraphic signature after basin formation. This signature may be either a change in pollen assemblage, or a switch from low to high organic production in the basins. By these criteria, 29 sites in this network (56%, Table 2) display a clear shift upsection in either pollen or organic content. This transition occurred over the broad range of 18.6 to 13 ka (Table 2, Fig. 3b). However, in more than half (N = 18) of these 29 sites transition occurred during a more constrained time period: the ~2.6 ka interval from 18.6 to 16 ka, with a peak at ~16.9 ka (Table 2).

Geographically, these 18 sites follow a general southwest to northeast trend (Fig. 4b). Bunnel Road (22) also demonstrates change within this time period, despite its southerly location. To the north, however, transitioning sites for this interval generally stop at ~41°N. Sedimentary changes continue after ~16 ka (Table 2, Fig. 3), and include sites in northern Indiana, and one in Michigan. The next noticeable peak occurs at ~13.2 ka. Three sites that are widespread throughout the study area undergo a transition at this time (Sites 19, N and S; Figs. 1 and 2). While we recognize that this sample size is quite small, the peak is worth noting it corresponds to the end of a regional pollen zone at 13.5 ka. This marks the onset of a warm period, as indicated by the decline in *Picea* spruce in favor of deciduous species (Shane, 1987). The Inter-Allerød Cooling Period (IACP) at 13.2 ka, as seen in Greenland, is also evident at Seneca Lake proxies in New York (Ellis et al., 2004).

Although the cause of a shift within an individual basin may vary, its occurance over a wide geographical area suggests larger-scale climatic forcing. Still, only 56% of sites include a transition at all, and only 29% of the total collection of basins exhibit change from 18.6 to 16 ka. A few reasons for this are discussed below.

Discussion

Do these basal and transition dates reflect regional events?

To assess whether the probability peaks from our raw data set are real (Fig. 3), we compared our results to a collection of radiocarbon ages that were randomly generated using the Monte Carlo method (Bevington and Robinson, 2003). To eliminate possible impacts from the non-linear calibration curve, we carried out this exercise in uncalibrated radiocarbon years. For both the basal and transition ages (Tables 1 and 2), samples were generated of the same respective sizes (N = 52 and N = 29) and the same age range as the observed data set. Since the shape of the resulting probability curve depends on the error of the individual ages, we applied the error values from the actual radiocarbon results to the randomly generated ages. With the random set and respective errors, the summed probability of the ^{14}C distribution was computed for 15,000 trials. The height of the tallest peak from each synthetic data set was then compared to the heights of the peaks in the observed radiocarbon data set.

For the basal formation, our tallest peak at ~15.5 ^{14}C ka BP was exceeded in five of the 15,000 trials, or 0.03% (an example of 500 trials is shown in Fig. 5a). The second highest peak, occurring at 14.5 ka ^{14}C ka BP, was exceeded in only 0.57% (N = 86) of those runs. In a similar exercise for the transition dates (Table 2), a run of fewer synthetic samples (200 total) showed that the highest peak was exceeded 38.5% of the time (Fig. 5b). This suggests that these peaks may not be statistically different from chance. In addition, this finding relates to the size of the peak, and not its temporal placement.

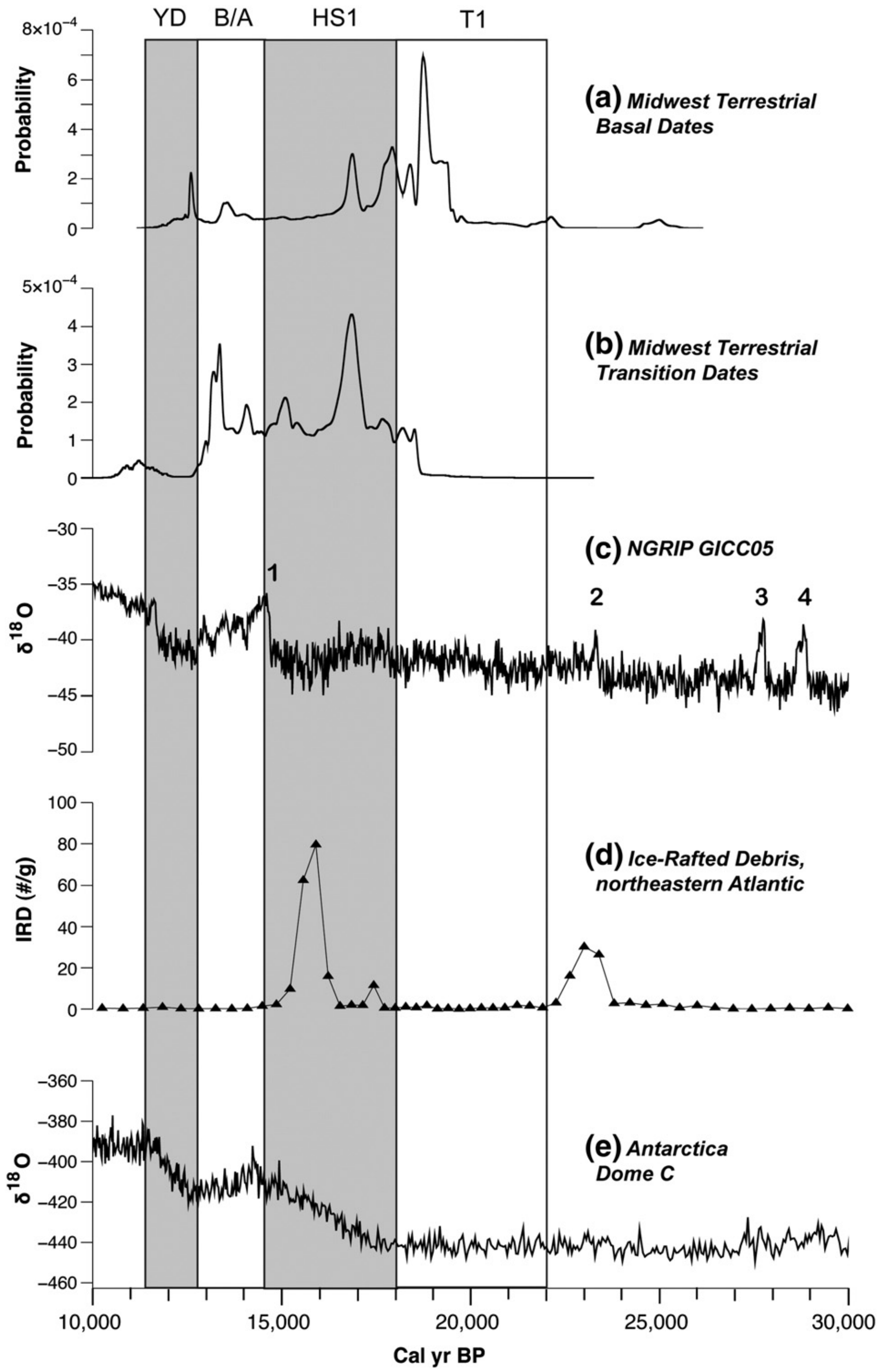

Figure 3. Summary of climate events during the last 30,000 years. Climatic events and their dates that are well-documented in the Northern Hemisphere are labeled in the background (Denton et al., 2010, unless otherwise noted). T1 = Termination 1 (22–18 ka), HS1 = Heinrich Stadial 1 (18–14.6 ka; Barker et al., 2009), H1 = Heinrich Event 1 (16.8 ka, Hemming, 2004), B/A = Bølling–Allerød (14.7–12.7 ka), IACP = Intra-Allerød Cold Period (13.4 ka), YD = Younger Dryas (12.8–11.5 ka). (a) Probability summation of converted bog-bottom dates (N = 52) from Ohio, Michigan and Indiana. (b) Probability summation of converted environmental transition dates (N = 29) from the Midwest. Transition events consist of significant organic, sedimentological or pollen changes in core sequences from small terrestrial basins. (c) Greenland ice core oxygen isotope data (Andersen et al., 2006; and Rasmussen et al., 2006). (d) EPICA Dome 3 Antarctica ice core oxygen isotope data (Parrenin et al., 2007). (e) Ice-rafted debris, including 150 μm diameter or larger carbonates and hematite from core location off the coast of Portugal (Bard et al., 2000).

This method provides only a loose assessment of the statistical significance of individual peaks. However, this exercise increases our confidence that the tallest peaks in our summed probability diagram for basal dates (Fig. 3a) represent real events. These basal dates cluster at certain times, indicating that terrestrial samples become available and preserved at preferred times.

Transitional dates, on the other hand, do not cluster in a way that would display a stronger signal than our randomly-generated sets. This is likely because the collection of sites that show a transition is only a subset of the entire collection (N = 29), and, as discussed, not all sites were ideal for recording an environmental change after deglaciation. Perhaps a more systematically collected data set could

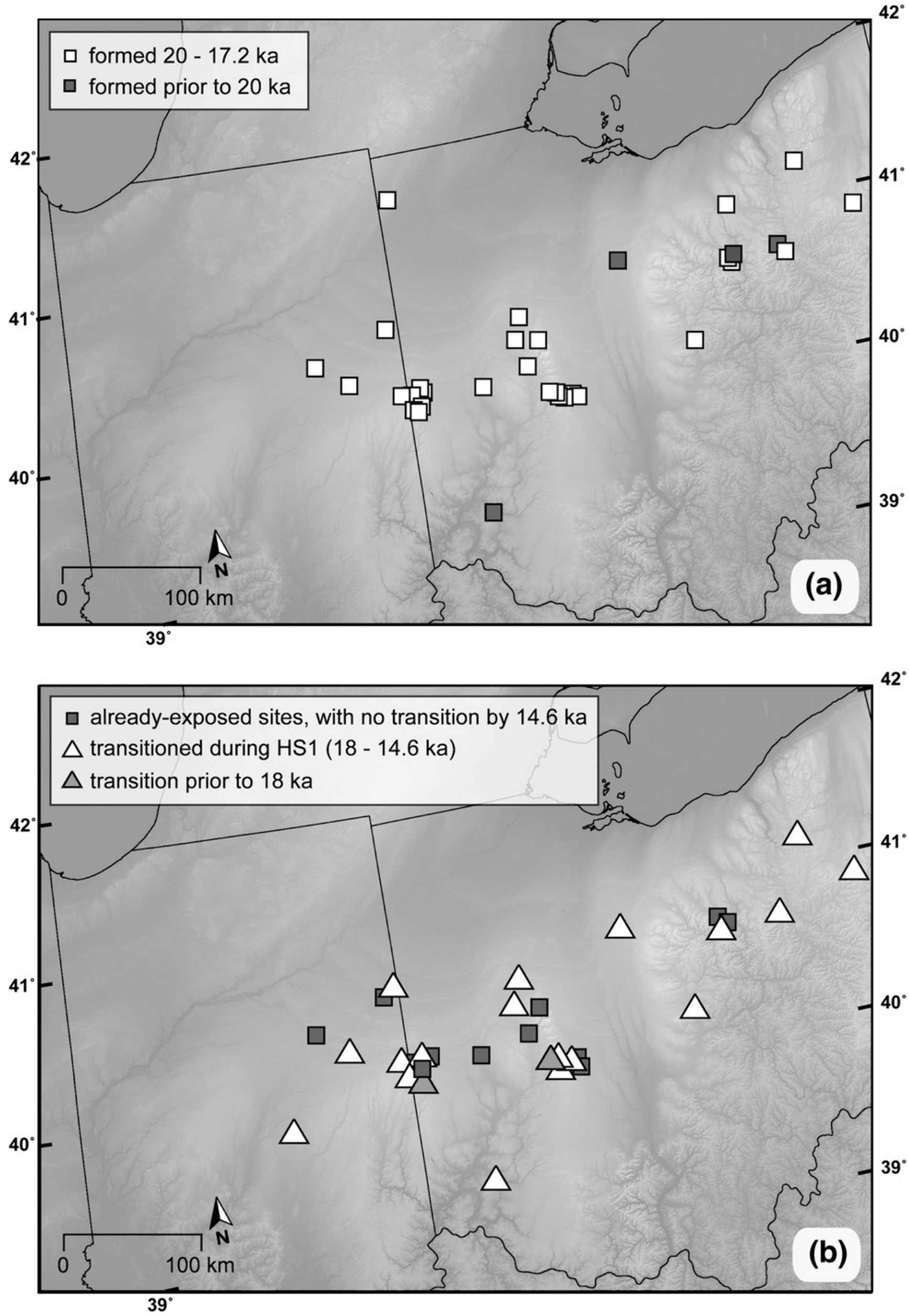

Figure 4. (a) First phase of widespread deglaciation and climate change, c. 20–17.2 ka. Sites exposed prior to 20 ka are noted in dark gray. (b) Sites that have formed and/or undergone an environmental transition during HS1.

link environmental change with the stratigraphic expression in lacustrine sections.

Usefulness of a multi-basin approach

We argue that our network of basal ages reflects regional deglaciation. As shown, individual examples may vary, but taken together, a network produces a consistent spatial pattern. We also recognize that of the 52 sites, only 29 contain records that display a distinct horizon of environmental change. Basins, particularly the small ones targeted in this study, may be extremely sensitive to local effects and geomorphological processes. It was not uncommon to see a sedimentary sequence that received clastic, inorganic sediment until the lake had filled. The record of the organic production of the lake is often an indicator of its response to climatic warming, but continuous surface drainage and deposition into the basin can "overprint" this. As a preliminary estimate, then, about one-half of the records here recorded distinct lithological changes at times that suggest more widespread climatic forcing. Regardless of the cause, future studies on regional scales may want to replicate basins in multiple settings.

Gradual change at the poles vs. episodic, rapid retreat of the ice-sheet margin

For illustration purposes, we make a preliminary contrast of the events recorded at the Laurentide Ice Sheet margin at ~40°N with the

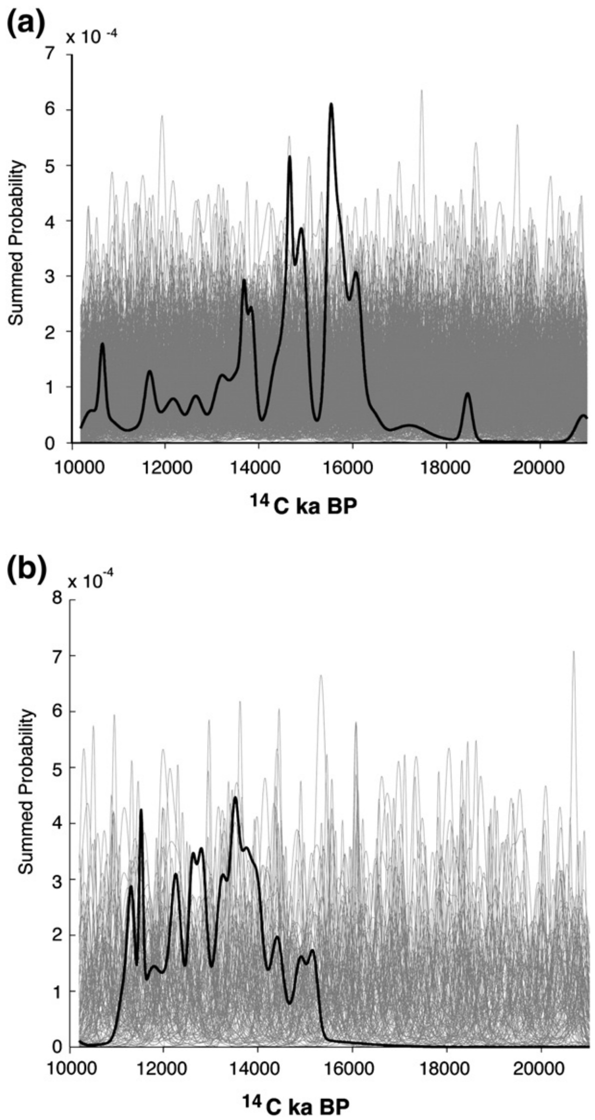

Figure 5. (a) Observed summed probability (thick line) from the radiocarbon ages that represent basal stratigraphic positions, compared with synthetic data sets (gray lines). Results described in the text are discussed in terms of 15,000 synthetic data sets; here, 500 sets are shown. Although a randomly generated set of ages could *potentially* yield the same probability as our observed set (particularly the peak at c. 15.5 ^{14}C ka BP), this rarely occurred. (b) A similar exercise for the transitional dates (thick line), and only 200 synthetic data sets, quickly shows that peaks from our observed data set have a greater chance (38.5% of cases) of replication.

polar and North Atlantic records. According to the North Atlantic isotope reference section developed from Greenland GRIP and NGRIP isotope records (Lowe et al., 2008), glacial conditions generally existed from 30.0 to 14.8 ka. This time period was punctuated with three short (~200–400 yr) interstadials starting at 28.9, 27.8 and 23.3 ka. The maximum glacial extent in Ohio has been dated to 23.2 ka, with moraines in both the Miami and Scioto sublobes that formed at the onset of a warm cycle (Lowell et al., 1990, 1995). The onset of deglaciation correlates well with Greenland Interstadial 2 at 23.3 ka (Svensson et al., 2008), and the presence of ice-rafted debris in the northeastern Atlantic at 23 ka (Bard et al., 2000). In Ohio, exposure of the Bunnel Road site (22) occurred shortly after at ~22 ka, indicating a pull-back of the ice margin while the ice cores show continuous cold conditions.

In North America, variations in northern summer insolation values may have forced the beginning of ice-sheet melting, collapse and retreat (Clark et al., 2009; Denton et al., 2010). Clark et al. (2009) note that 10 W m^{-2} above the minimum represents a threshold where an ice sheet's mass balance will start declining. In the North American Midwest, the demise of the Laurentide continued after 23.2 ka, while the isotope signal indicates a return to prior, full-glacial levels in Greenland. Only gradual change occurs in the isotope record from 23.2 to 18 ka, on the order of 6 per mil in δ^{18}O at NGRIP (Svensson et al., 2008). There is no return to interstadial-level isotope values as the Laurentide Ice Sheet retreated ~100 km in the Midwest. A pattern of similar events occurred in areas northeast of our study region. In New England, the Martha's Vineyard moraine demarcated the maximum extent of the local ice-sheet margin at ~23.7 ka (Balco et al., 2002). Southeastern Connecticut was deglaciated between 21.0 and 20.5 ka, and another episode of moraine emplacement and warming occurred at 18.5 ka in New England (Balco et al., 2002; Balco and Schaefer, 2006; Balco et al., 2009). A record of summer insolation values at 40°N (Fig. 6) shows a detectable increase that begins 19 to 18.5 ka. Warming was then detected in the Finger Lakes region of New York by ~16.6 ka (Ellis et al., 2004).

Despite the onset of Midwestern deglaciation correlating well with Northern Hemisphere warming at 23.2 ka, the environmental conditions required to sustain this first major retreat of Laurentide Ice Sheet for the next 5 ka is not apparent in the polar ice record. It may be that the isotope record is not a suitable analog for ice-sheet forcing. This has been noted for events in the Holocene, where known warming events at Summit, Greenland are not reflected in local isotope data due to shifts in precipitation sources (LeGrande and Schmidt, 2009). During the period of apparent stability (23.3–14.8 ka), precipitation delivery may have been altered because of larger changes in Earth's atmospheric circulation, perhaps due, in part, to the presence of the Larentide Ice Sheet over North America. This is also a time of low accumulation rates on the Greenland Ice Sheet (van der Veen, 2002).

In the case of the South Pole, Antarctic isotope data also shows little change from full-glacial conditions during this time (Fig. 3e). The onset of gradual isotopic increase does not occur until 17.5 to 17.0 ka (Anderson et al., 2009). Neither of the records from the poles predict the pattern of ice-sheet retreat documented here.

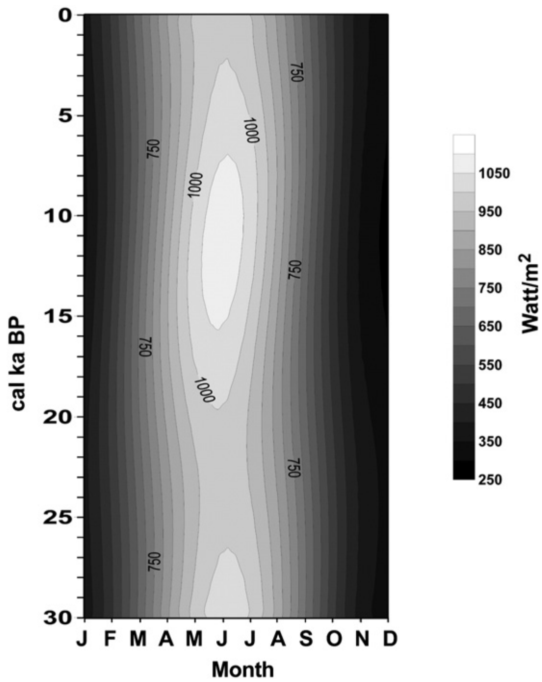

Figure 6. Average monthly insolation values for 40° N contoured in W/m^2 (Berger and Loutre, 1991). Note that by 18.9 ka the summer values, which are key for ablation, have risen.

Between 18.6 and 13.0 ka in the Midwest, about half of sites in our study area either 1) received increased pollen input or evidence of more temperate species, or 2) switched from inorganic sedimentation to organic, autochthonous production. Of those sites that show a transition, many cluster during a widespread phase of warming between 18.6 and 16.0 ka, with a peak at ~16.8 ka. This precedes major North Atlantic episodes that are reflected in ice rafted debris at ~16 ka (Bard et al., 2000; Fig. 3e), and Greenland Interstadial 1 at ~14.8 ka (Svensson et al., 2008). This suggests that some modulation in the climate signal is operating outside the high latitudes.

The discrepancy between terrestrial and polar records is not a new phenomenon; Denton et al. (2006) describe a mystery interval from 17.5 to 14.5 ka, synchronous with Heinrich Stadial 1, as a period when the nature of terrestrial mid-latitude warming is at odds with ocean records that demonstrate cooling and an increase in winter sea ice (Denton et al., 2010). In particular, significant recession of alpine glaciers worldwide (e.g. the Swiss Alps, Sierra Nevada, Andes, and New Zealand) occurred in synchronicity about 18 ka, suggesting a widespread, interhemispheric forcing mechanism, such as increased insolation and summer temperatures (Schaefer et al., 2006). Meanwhile, sea surface temperatures (SST) in the Mediterranean and North Atlantic dropped between 17.8 and 15 ka. Our data indicate sufficient warming to force the ice-sheet margin back prior to the mystery interval. Denton et al. (2010) suggest that the significant input of meltwater into the oceans that could only come from the collapse of massive ice sheets may have resulted in the drop in SST, weaker North Atlantic turnover, and then increased winter sea-ice cover in polar areas. Although it remains to be seen if other margins are responding, meltwater lost from North America to the North Atlantic may have allowed the Arctic Ocean to maintain colder conditions for thousands of years to come.

By 12 ka, all sites in our study area were deglaciated. Likely, the ice sheet had retreated entirely from the region, marking the end of the Last Termination at 11.5 ka (Lowe et al., 2008).

Conclusions

1) Taken together, multiple sites suggest that deglaciation of the east-central sector of the Laurentide Ice Sheet occurred shortly after emplacement of LGM moraines at 23.3 ka. This time is earlier than generally believed for North America, where the onset of deglaciation is estimated at 20 to 19 ka (Clark et al., 2009; Denton et al., 2010). The extent of this retreat is documented by multiple sites (N = 52) throughout Ohio and Indiana that form between 20.0 and 17.2 ka, many of which are located ~100 km inside the LGM limit.
2) Our data set suggests later warming events for the region at 16.8 and 13.2 ka, but we have low confidence that these events are real. This is likely due, in part, to the localized effects that can occur at small lake basins. Further work is needed to define the exact nature, timing, and extent of these events.
3) Discrepancies between the apparent onset of deglaciation in central Greenland and in New England, the Midwest, and the North Atlantic hint at the limitation of oxygen isotope data as a direct proxy for ice sheet forcing. This is consistent with the nature of the oxygen isotope record, which is strongly influenced by other factors. Rising summer insolation may be the most important forcing for this early deglaciation in the continental mid-latitudes (Fig. 6; Berger and Loutre, 1991; Clark et al., 2009).

Acknowledgments

Detailed comments from two anonymous reviewers greatly improved the manuscript. Funding was provided by the Comer Science and Education Foundation, W. M. Keck Foundation, Geological Society of America, The National Academies, and Sigma Xi Society. Assistance for fieldwork included participants of the Keck Glacial Ohio 2001–2002 field seasons, Benjamin Jones, Sam Donaldson, Katie Pritchard, Alexander Stewart, Michelle Hart, Joshua Michaels, Janelle Sikorski, Cathy Licht, and Jennifer Nelson. AMS facilities used in this study include the University of Arizona, Beta Analytic, Inc., and ETH/PSI AMS Facility in Zurich. John Nicol and Bill Glover provided feedback and encouragement on the final draft.

References

Andersen, K.K., Svensson, A., Johnsen, S.J., Rasmussen, S.O., Bigler, M., Röthlisberger, R., Ruth, U., Siggaard-Andersen, M.L., Steffensen, J.P., Dahl-Jensen, D., Vinther, B.M., Clausen, H.B., 2006. The Greenland ice core chronology, 15–42 kyr. Part 1: constructing the time scale. Quaternary Science Reviews 25, 3246–3257.

Anderson, R.F., Ali, S., Bradtmiller, L.I., Nielson, S.H.H., Fleisher, M.Q., Anderson, B.E., Burckle, L.H., 2009. Wind-driven upwelling in the Southern Ocean and the deglacial rise in atmospheric CO_2. Science 323, 1443–1448.

Bailey, R.E., 1972. Late- and postglacial environmental changes in northwestern Indiana. Dissertation. Indiana University, Bloomington, Indiana, USA.

Balco, G., Schaefer, J.M., 2006. Cosmogenic-nuclide and varve chronologies for the deglaciation of southern New England. Quaternary Geochronology 1, 15–28.

Balco, G., Stone, J.O.H., Porter, S.C., Caffee, M.W., 2002. Cosmogenic-nuclide ages for New England coastal moraines, Martha's Vineyard and Cape Cod, Massachusetts, USA. Quaternary Science Reviews 21, 2127–2135.

Balco, G., Briner, J., Finkel, R.C., Rayburn, J.A., Ridge, J.C., Schaefer, J.M., 2009. Regional beryllium-10 production rate calibration for late-glacial northeastern North America. Quaternary Geochronology 4, 93–107.

Bard, E., Rostek, F., Turon, J., Gendreau, S., 2000. Hydrological Impact of Heinrich Events in the Subtropical Northeast Atlantic. Science 289, 1321–1324.

Barker, S., Diz, P., Vautravers, M.J., Pike, J., Knorr, G., Hall, I.R., Broecker, W.S., 2009. Interhemispheric Atlantic seesaw response during the last deglaciation. Nature 457, 1097–1101.

Berger, A., Loutre, M.F., 1991. Insolation values for the climate of the last 10 million years. Quaternary Science Reviews 10 (4), 297–317.

Bevington, P., Robinson, D.K., 2003. Data Reduction and Analysis for the Physical Sciences. McGraw Hill, St. Louis.

Cheng, H., Edwards, L., Broecker, W.S., Denton, G.H., Kong, X., Wang, Y., Zhang, R., Wang, X., 2009. Ice Age Terminations. Science 326, 248–252.

Clark, P.U., Dyke, A.S., Shakun, J.D., Carlson, A.E., Clark, J., Wohlfarth, B., Mitrovica, J.X., Hostetler, S.W., McCabe, A.M., 2009. The last glacial maximum. Science 325 (5941), 710–771.

Clayton, L., Moran, S.R., 1983. Chronology of late Wisconsinan Glaciation in Middle North America. Quaternary Science Reviews 1, 55–82.

Dean, W.E., 1974. Determination of carbonate and organic matter in calcareous sediments and sedimentary rocks by loss on ignition: comparison with other methods. Journal of Sedimentary Petrology 44 (1), 242–248.

Denton, G.H., Heusser, C.J., Lowell, T.V., Moreno, P.I., Andersen, B.G., Heusser, L.E., Schluchter, C., Marchant, D.R., 1999. Interhemispheric linkage of paleoclimate during the last glaciation. Geografiska Annaler, Series A: Physical Geography 81, 107–153.

Denton, G.H., Broecker, W.S., Alley, R.B., 2006. The mystery interval 17.5 to 14.5 kyrs ago. PAGES News 14, 14–16.

Denton, G.H., Anderson, R.F., Toggweiler, J.R., Edwards, R.L., Schaefer, J.M., Putnam, A.E., 2010. The last glacial termination. Science 328, 1652–1656.

Ellis, K.G., Mullins, H.T., Patterson, W.P., 2004. Deglacial to middle Holocene (16,600 to 6000 calendar years BP) climate change in the northeastern United States inferred from multi-proxy stable isotope data, Seneca Lake, New York. Journal of Paleolimnology 31, 343–361.

Glover, K.C., 2004. Paleoenvironmental Evidence for the Last Termination in two bog sequences and a Regional Network of sites from Ohio and Eastern Indiana. Master's Thesis. University of Cincinnati, Cincinnati, Ohio, USA.

Hemming, S.R., 2004. Heinrich events: massive Late Pleistocene detritus layers of the North Atlantic and their global imprint. Reviews of Geophysics 42, 1–43.

Heusser, L., Maenza-Gmelch, T., Lowell, T., Hinnefeld, R., 2002. Late Wisconsin periglacial environments of the southern margin of the Laurentide Ice Sheet reconstructed from pollen analyses. Journal of Quaternary Science 17, 773–780.

Hinnefeld, R., 1996. The eolian component of last glacial maximum lacustrine sediment; the Bunnel Road site in Southwest Ohio. Master's Thesis. University of Cincinnati, Cincinnati, Ohio, USA.

LeGrande, A.N., Schmidt, G.A., 2009. Sources of Holocene variability of oxygen isotopes in paleoclimate archives. Climate of the Past 5, 441–455.

Lowe, J.J., Rasmussen, S.O., Björck, S., Hoek, W.Z., Steffensen, J.P., Walker, M.J.C., Yu, Z.C., the INTIMATE group, 2008. Synchronisation of paleoenvironmental events in the North Atlantic region during the Last Termination: a revised protocol recommended by the INTIMATE group. Quaternary Science Reviews 27, 6–17.

Lowell, T.V., 1995. The application of radiocarbon age estimates to the dating of glacial sequences: an example from the Miami sublobe, Ohio, U.S.A. Quaternary Science Reviews 14, 85–99.

Lowell, T.V., Savage, J.M., Brockman, C.S., Stuckenrath, R., 1990. Radiocarbon Analyses from Cincinnati, Ohio and Their Implications for Glacial Stratigraphic Interpretations. Quaternary Research 34, 1–11.

Lowell, T.V., Heusser, C.J., Andersen, B.G., Moreno, P.I., Hauser, A., Heusser, L.E., Schluchter, C., Marchant, D.R., Denton, G.H., 1995. Interhemispheric correlation of late pleistocene glacial events. Science 269, 1541–1549.

Ogden, J.G., 1966. Forest History of Ohio. I. Radiocarbon Dates and Pollen Stratigraphy of Silver Lake, Logan County, Ohio. Ohio Journal of Science 66, 387–400.

Overpeck, J.T., Webb III, T., Prentice, I.C., 1985. Quantitative interpretation of fossil pollen spectra: dissimilarity coefficients and the method of modern analogs. Quaternary Research 23 (1), 87–108.

Parrenin, F., Loulergue, L., Wolff, E., 2007. EPICA Dome C Ice Core Timescales EDC3. IGBP PAGES/World Data Center for Paleoclimatology Data Contribution Series # 2007–083. NOAA/NCDC Paleoclimatology Program, Boulder CO, USA.

Porter, S.C., Carson, R.J., 1971. Problems of interpreting radiocarbon dates from dead-ice terrain, with an example from the Puget Lowland of Washington. Quaternary Research 1, 410–414.

Pritchard, K.L., 2006. Relationships and patterns of channel formation during deglaciation of the Miami Lobe, near Piqua, Ohio. Master's Thesis. University of Cincinnati, Cincinnati, Ohio, USA.

Rasmussen, S.O., Andersen, K.K., Svensson, A.M., Steffensen, J.P., Vinther, B.M., Clausen, H.B., Siggaard-Andersen, M.L., Johnsen, S.J., Larsen, L.B., Dahl-Jensen, D., Bigler, M., Röthlisberger, R., Fischer, H., Goto-Azuma, K., Hansson, M.E., Ruth, U., 2006. A new Greenland ice core chronology for the last glacial termination. Journal of Geophysical Research 111, D06102.

Reimer, P.J., Baillie, M.G.L., Bard, E., Bayliss, A., Beck, J.W., Blackwell, P.G., Bronk Ramsey, C., Buck, C.E., Burr, G., Edwards, R.L., Friedrich, M., Grootes, P.M., Guilderson, T.P., Hajdas, I., Heaton, T.J., Hogg, A.G., Hughen, K.A., Kaiser, K.F., Kromer, B., McCormac, F.G., Manning, S.W., Reimer, R.W., Richards, D.A., Southon, J., Turney, C.S.M., van der Plicht, J., Weyhenmeyer, C., 2009. IntCal09 and Marine09 radiocarbon age calibration curves, 0–50,000 years cal BP. Radiocarbon 51, 1111–1150.

Schaefer, J.M., Denton, G.H., Barrell, D.J.A., Ivy-Ochs, S., Kubik, P.W., Andersen, B.G., Phillips, F.M., Lowell, T.V., Schlüchter, C., 2006. Near-synchronous interhemispheric termination of the last glacial maximum in mid-latitudes. Science 312 (5779), 1510–1513.

Shane, L.C.K., 1975. Palynology and radiocarbon chronology of Battaglia Bog, Portage County, Ohio. Ohio Journal of Science 72 (2), 96–102.

Shane, L.C.K., 1987. Late-glacial vegetational and climatic history of the Allegheny Plateau and the Till Plains of Ohio and Indiana, U.S.A. Boreas 16, 1–20.

Shane, L.C.K., 1989. Changing palynological methods and their role in three successive interpretations of the late-glacial environments at Bucyrus Bog, Ohio, USA. Boreas 18, 297–309.

Shane, L.C.K., Anderson, K.H., 1993. Intensity, gradients, and reversals in late glacial environmental change in east-central North America. Quaternary Science Reviews 12, 307–320.

Singer, D.K., Jackson, S.T., Madsen, B.A., Wilcox, D.A., 1996. Differentiating climatic and successional influences on long-term development of a marsh. Ecology 77, 1765–1778.

Stuiver, M., Reimer, P.J., 2010. Calib 6.0. Belfast, Northern Ireland: calib.org Retrieved from calib.qub.ac.uk/calib/calib.html.

Svensson, A., Andersen, K.K., Bligler, H.B., Dahl-Jensen, D., Davies, S.M., Johnsen, S.J., Muscheler, R., Parrenin, F., Rasmussen, S.O., Röthlisberger, R., Seierstad, I., Steffensen, J.P., Vinther, B.M., 2008. A 60 000 year Greenland stratigraphic ice core chronology. Climate of the Past 4, 47–57.

van der Veen, C.J., 2002. Polar ice sheets and global sea level: how well can we predict the future? Global and Planetary Change 32, 165–194.

Whitehead, D.R., Jackson, S.T., Sheehan, M.C., Leyden, B.W., 1982. Late-Glacial vegetation associated with caribou and mastodon in central Indiana. Quaternary Research 17, 241–257.

Williams, A.S., 1974. Late-glacial–postglacial vegetational history of the Pretty Lake region, northeastern Indiana. U.S. Geological Survey Professional Paper 686-B. U.S. Government Printing Office, Washington, D.C., USA.